Noname manuscript No.
(will be inserted by the editor)

Proposal of a new method for strength evaluating of construction of railway vehicles

optimization of hood of diesel electric locomotive

Petr Tomek · Doubravka Středová

Received: date / Accepted: date

Abstract This article presents two methods for evaluating the strength of the hood of railway locomotives. The hood is subject to the European standards for railway applications EN 12663-1 [1]. The first method is anchored in the European standard for railway applications EN 12663-1 [1]. This method is based on the principle of evaluation of the pseudo-elastic stress. The second method uses the results of geometrically and materially nonlinear numerical analyzes. The second method is based on the knowledge of modern science and technology. Structural strength is then evaluated from the real limit state. Using of both methods for strength evaluating is shown in this paper (strength evaluation of hood of diesel electric locomotive). The original construction of hood is analyzed in the first part of this paper. Structural changes are proposed in the next part of this article. Carrying capacity of the new construction of hood is verified by a numerical analysis. The results of the new construction are compared with the original construction of hood

Keywords limit state of plasticity · railway applications · FEM · strength evaluation

List of symbols

a ... acceleration $[\mathrm{ms}^{-2}]$
a_{ALL} ... allowable acceleration $[\mathrm{ms}^{-2}]$
a_L ... limit acceleration $\left[\mathrm{ms}^{-2}\right]$
a_x ... acceleration in the direction of x axis $\left[\mathrm{ms}^{-2}\right]$
E... Young's modulus in tension $\left[\mathrm{Nmm}^{-2}\right]$
E_T... tangent modulus $\left[\mathrm{Nmm}^{-2}\right]$
f_y ... yield strength $\left[\mathrm{Nmm}^{-2}\right]$
f_u... ultimate strength $\left[\mathrm{Nmm}^{-2}\right]$
g ... acceleration of gravity $\left[\mathrm{ms}^{-2}\right]$
S_1... safety factor given the yield strength [1]
S_2... safety factor given the ultimate strength [1]
S_3... safety factor for loss of stability [1]
S_f... fictitious safety factor [1]
T... calculation temperature [°C]
W_{pl}... plastic cross section modulus in bending $\left[\mathrm{mm}^3\right]$
W_{el}... elastic cross section modulus in bending $\left[\mathrm{mm}^3\right]$

Greek symbols

μ ... Poissons number [−]
σ_{ALL} ... allowable elastic stress $[\mathrm{Nmm}^{-2}]$
σ_{int} ... reduced stress by hypothesis Tresca $\left[\mathrm{Nmm}^{-2}\right]$

P. Tomek
Department of Mechanics, Materials and machine Parts, University of Pardubice, Pardubice 53210, Czech Republic
Tel.: +420 466036484
E-mail: petr.tomek@upce.cz

D. Středová
Department of Mechanics, Materials and machine Parts, University of Pardubice, Pardubice 53210, Czech Republic

1 Introduction

Research task was to develop a new method for evaluation of strength in railway applications. Current method (anchored in EN 12663[1]) is not suitable for use in combination with modern computer technology. The new method is demonstrated in calculation the original and new construction of the hood of diesel electric locomotive. The next aim is to performed optimization of construction on the basis of the results of numerical analyses.

The original and new construction of the hood of diesel electric locomotive are analyzed in this paper. The original construction of hood is analyzed in the first part of this paper. Structural changes are proposed in the next part of this article. The changes are designed

on the basis of the results of numerical analyses. The critical points were detected in locations of rectangular tubes with a low carrying capacity. Carrying capacity of the new construction is verified by a numerical analysis. The results of the new construction are compared with the original construction of hood.

The whole construction is loaded by inertia effects caused by prescribed acceleration. The parts of the hood are subject to the European standard for railway applications EN 12663-1 [1]. Numerical analyses are performed by FEM computer program COSMOSWorks [2].

The strength of hood is evaluation by two methods. The first methodology is anchored in European standard EN 12663-1 [1]. The second methodology is nonlinear numerical analysis GMNA (Geometrically and Materially Nonlinear Analysis). The second methodology is applied to basis of methods of modern science and technology. The results are evaluated according to EN 12663-1 [1] and EN 1993 [3].

2 Coordinate system and loads

The coordinate system is taken from EN 12663-1 (see Figure 1). Numerical models are subjected to acceleration in specified directions. Acceleration values are given in Table 1.

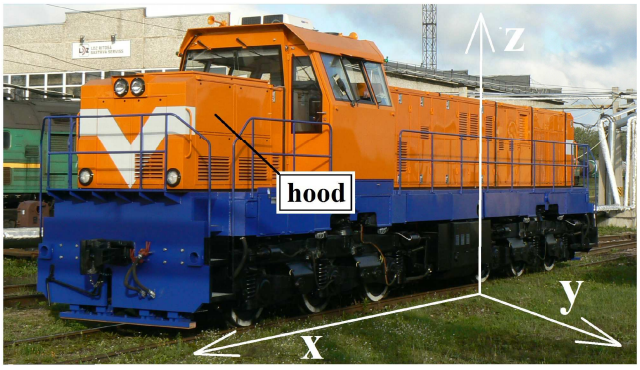

Fig. 1 Coordinate system according to EN 12663-1

The principle and procedure of evaluating the strength of hood is the same for all load cases (see Table 1). Detailed descriptions of evaluation of the strength of the hood is shown only for load case LC2 in this paper. The results (allowable and limit loads) for the other load cases are given in tables hereafter in the article.

3 Methodology anchored in EN 12663-1

The methodology anchored in EN 12663-1 [1] is based on a linear static analysis. Calculated pseudo - elastic stresses are compared with allowable stress. This methodology does not assess correctly the influence of stress concentrations (notches, changes in geometry, etc.) for strength of construction and it cannot detect any loss of stability. Therefore the results obtained by method according to EN 12663-1 [1] are only approximate. The definite conclusion cannot be derived from these results. Allowable elastic stress is determined by following condition:

Table 1 The limit value of components of acceleration according to EN 12663-1 ($g = -9.81\,\mathrm{ms}^{-2}$).

load case (LC)	x-axis	y-axis	z-axis
1	0	0	$3g$
2	$-3g$	0	$1g$
3	0	$-1g$	$1g$

$$\sigma_{ALL} = \min\left(\frac{f_y}{S_1}; \frac{f_u}{S_2}\right) \tag{1}$$

Where

- $f_y\,[\mathrm{Nmm}^{-2}]$ ... yield strength,
- $f_u\,[\mathrm{Nmm}^{-2}]$ ... ultimate strength,
- $S_1 = 1.15$ ... safety factor given the yield strength,
- $S_2 = 1.5$ ... safety factor given the ultimate strength.

Equivalent (reduced) stress according to the hypothesis of maximum shear stress (Tresca, intensity) σ_{int} is used for evaluation of strength. European standard EN 12663-1 [1] does not distinguish surface of the shell element (TOP, MIDDLE, BOTTOM). Stress is conservatively evaluated on the surfaces TOP and BOTTOM. Conditions of strength according to EN 12663-1 [1] are:

1. The calculated stress in the numerical model σ_{int} cannot exceed the allowable elastic stress σ_{ALL}.
2. Calculated pseudo - elastic stress can exceed yield stress f_y in the local stress concentrations. Areas with permanent deformations due to local stress concentrations must be sufficiently small. Significant permanent deformation cannot occur after the end of the load.

Detailed example the using of the first methodology anchored in EN 12663-1 [1] is given in next Chapter.

3.1 Evaluation of original construction

Methodology specified in EN 12663-1 [1] is used for evaluation of strength of the original construction of hood in this chapter. Original construction is made from a material S275J2H. Mechanical properties for material S275J2H are shown in Table 2.

Table 2 Mechanical properties of material S275J2H

T [°C]	E [Nmm^{-2}]	f_y [Nmm^{-2}]	f_u [Nmm^{-2}]
20	2.01E+5	275	430

Allowable stress is determined by following condition:

$$\sigma_{ALL} = \min\left(\frac{f_y}{S_1}; \frac{f_u}{S_2}\right) = \min\left(\frac{275}{1.15}; \frac{430}{1.5}\right) = \\ = \min\left(239.13; 286.67\right) = 239.13\,\mathrm{Nmm}^{-2} \quad (2)$$

Where

- $f_y = 275\,\mathrm{Nmm}^{-2}$ ... yield strength (S275J2H),
- $f_u = 430\,\mathrm{Nmm}^{-2}$ ... ultimate strength (S275J2H),
- $S_1 = 1.15$ ... safety factor given the yield strength,
- $S_2 = 1.5$ ... safety factor given the ultimate strength.

The computational model of hood is very large and complex. The individual connections of tubes (structural nodes) are evaluated separately. Identification of all connections is shown in the Figures 2, 3 and 4.

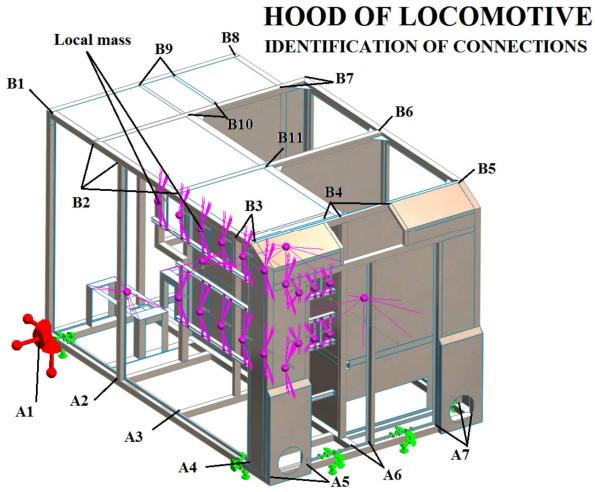

Fig. 2 Identification of connections - upper part of the hood

The computational model is shown in Figure 5. FEM mesh is created by parabolic shell-elements SHELL6T (Figures 6 and 8). The mesh is softened at controlled connection. The rest of construction contains a loose mesh. For each connections and selected load cases (Table 1) were performed numerical linear static analyses. Example of evaluation of connections A9 and B10 for load case LC2 is shown in Figures 7 and 9.

Deformed model with drawn a reduced stress Tresca on the TOP surface is shown in Figures 7 and 9. The

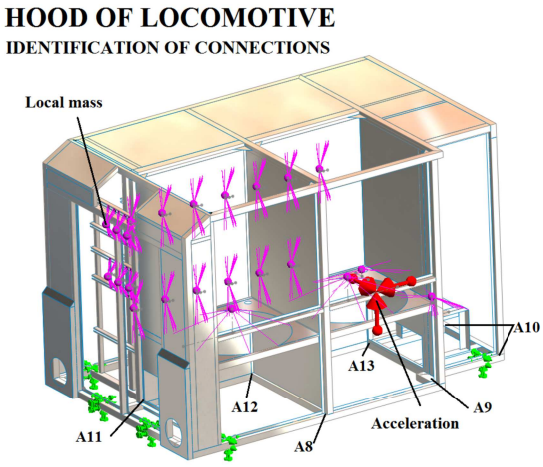

Fig. 3 Identification of connections - lower part of the hood

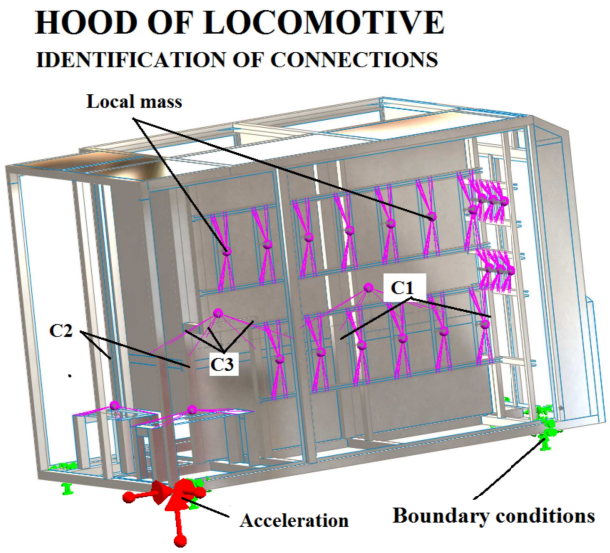

Fig. 4 Identification of connections - middle part of the hood

red - colored areas are clearly visible on the numerical model. The reduced stress σ_{int} exceeded the allowable stress $\sigma_{ALL} = 239\,\mathrm{Nmm}^{-2}$ in this areas.

4 Nonlinear analysis (GMNA) and safety factor

Geometrically and materially nonlinear analysis (GMNA) is the basis of the second methodology. Numerical analyses GMNA are performed by FEM computer program COSMOSWorks [2]. The real limit state (loss of stability, plasticity limit state) is the result of non-linear numerical analysis. The strength of construction is evaluated from the limit load, when it occurs the real limit state. This method is commonly used for the design of restricted equipment (e.g. pressure vessels, steel structures, etc.) in the energy, chemical, nuclear and trans-

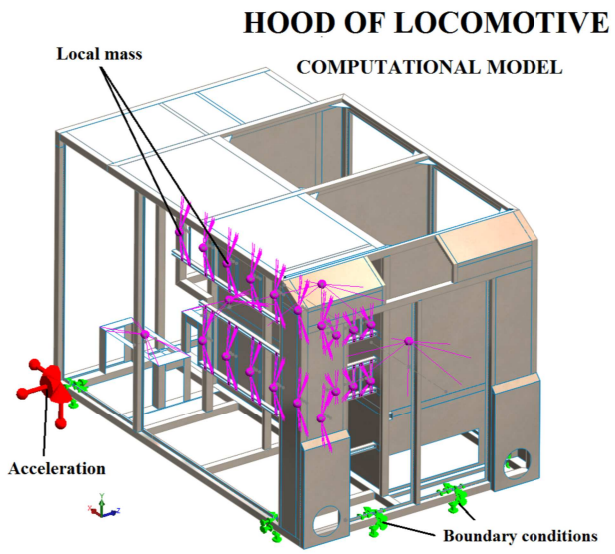

Fig. 5 Computational model

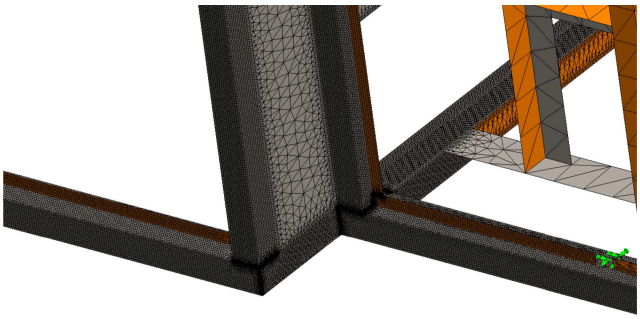

Fig. 6 Connection A9 - detail of FEM Mesh

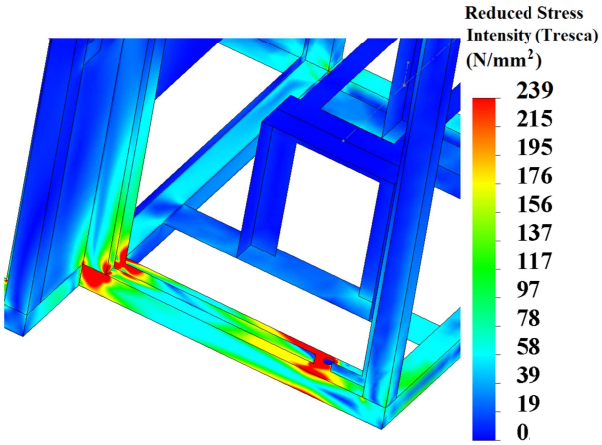

Fig. 7 Connection A9 - Reduced stress Tresca (LC2)

portation industries. Two nonlinearities (geometric and material) are considered in numerical analyses. Geometric nonlinearity (large displacements) allows for the detection the loss of stability of the structure. Material nonlinearity takes into account elastic - plastic material behavior (plasticity). The von Mises's bilinear model of

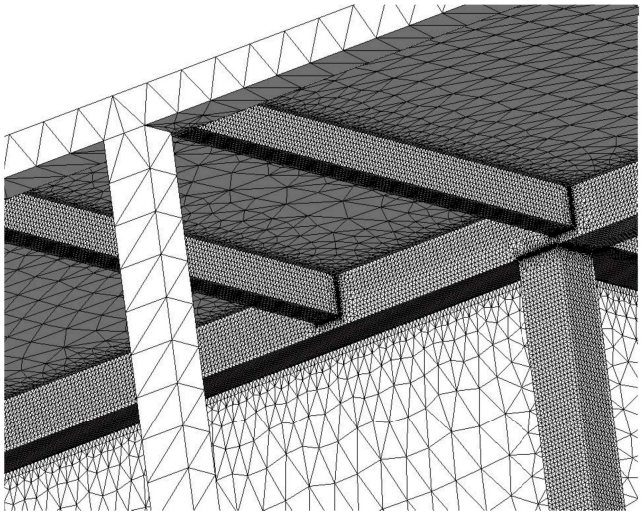

Fig. 8 Connection B10 - detail of FEM Mesh

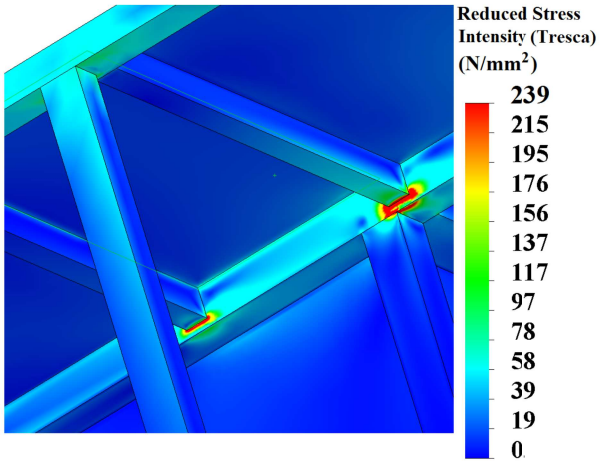

Fig. 9 Connection B10 - Reduced stress Tresca (LC2)

elastic - plastic material behavior with Young's modulus $E = 2E + 5\,\mathrm{Nmm}^{-2}$ (for carbon steel), Poisson's number $\mu = 0.3$ (for carbon steel), yield strength f_y and tangent modulus (isotropic hardening) $E_T = E/10000$ is used in the numerical analyses GMNA.

The following safety factors are indicated in EN 12663-1 [1]:

- $S_1 = 1.15$ ... Safety factor for yield strength,
- $S_2 = 1.50$ ... Safety factor for ultimate strength,
- $S_3 = 1.50$ ... Safety factor for loss of stability.

The standard EN 12663-1 [1] recommends the use of increased levels safety factor S_1 for evaluating the results of nonlinear analysis (GMNA). However value of the safety factor S_1 for the use of numerical analysis GMNA is missing. Safety factor S_1 is determined for evaluating strength of construction on the basis of the pseudo-elastic stress. Limit state is determined by allowable elastic stress σ_{ALL}.

$$\sigma_{ALL} = \min\left(\frac{f_y}{S_1}; \frac{f_u}{S_2}\right) \tag{3}$$

The real limit state of plasticity occurs after the establishment of a sufficient number of plastic hinges. Then the construction behaves as kinematic mechanism. The real limit state is the result of non-linear numerical analysis GMNA. Safety factor $S = 1.5$ is used to evaluate the structural strength for the limit state of plasticity. Safety factor $S = 1.5$ is based on increased levels of safety factor S_1. Value of safety factor $S = 1.5$ is based on the methods for evaluating the strength of steel construction from the real limit state of plasticity. But the safety factor $S = 1.5$ does not include affect thin wall of rectangular tubes on the limit state of plasticity. The ratio between the elastic and plastic cross section modulus in bending is $\eta_1 = 1.5$ for solid rectangular cross-section.

$$\eta_1 = \frac{W_{pl1}}{W_{el1}} = 1.5 \tag{4}$$

Where

- $W_{pl1}\,[\mathrm{mm}^3]$ ... plastic modulus in bending,
- $W_{el1}\,[\mathrm{mm}^3]$ ... elastic modulus in bending.

The ratio between the elastic and plastic cross section modulus in bending η_2 is from 1.15 to 1.18 for thin wall rectangular tubes.

$$\eta_2 = \frac{W_{pl2}}{W_{el2}} \tag{5}$$

Safety factor $S = 1.5$ should be added to the influence of thin wall rectangular tubes. Fictitious safety factor S_f takes into account low reserve of carrying capacity of thin wall profile. Fictitious safety factor S_f is based on safety factor $S = 1.5$ and it is determined by the following equation.

$$S_f = S \cdot \frac{\eta_1}{\eta_2} = 1.5 \cdot \frac{1.5}{1.15} = 1.956 \tag{6}$$

$$S_f = 2 \tag{7}$$

Fictitious safety factor $S_f = 2$ and using of nonlinear numerical analysis GMNA are not anchored in EN 12663-1 [1]. Application of nonlinear analysis GMNA together with fictitious safety factor S_f for the evaluation of the hood is based on current knowledge of science and technology. Computational dimension of welds can not be less than the thickness of connected profiles. Then evaluation of the strength on the basis of numerical analysis GMNA and fictitious safety factor S_f is also valid for welded connections. Strength check of the welds must be performed if the welds have a lower computational dimension than the thickness of the connected profiles. Detailed example of the using the second methodology (numerical analyses GMNA) is given further.

4.1 Nonlinear numerical analysis GMNA - original construction

The limit acceleration for load case LC2 of the numerical model is found in this chapter. The computational model is shown in Figure 10. Local masses (contactors, cooling units) are prescribed by mass elements. FEM mesh is created by shell element SHELL6T (see Figure 11). The numerical model is exposed to acceleration $a_x = 3 \cdot g = 29.43\,\mathrm{ms}^{-2}$ ($g = 9.81\,\mathrm{ms}^{-2}$) and $a_z = 1 \cdot g = 9.81\,\mathrm{ms}^{-2}$. Numerical model is fixed in the location for bolts. The von Mises's bilinear model of elastic - plastic material behavior with Young's modulus $E = 2E + 5\,\mathrm{Nmm}^{-2}$, Poisson's ratio $\mu = 0.3$, yield strength $f_y = 275\,\mathrm{Nmm}^{-2}$ (see Tab. 2) and tangent modulus (isotropic hardening) $E_T = E/10000$ is used in the numerical analyses GMNA. The equilibrium curve (see Figure 12) is the ratio of the load factor LF (load multiple of computational load) and the total displacement of the selected node ND 18125 (see Figure 12). The numerical model has a linear behavior until the load factor $LF \sim 1.1$. Plastic hinges begin to develop after reaching this point. Establishment and development of plastic hinges is accompanied by a decrease stiffness of the construction. Limit state of plasticity is reached in the 41^{th} step. The value of limit load factor is $LF_L = 1.83$. Deformed model with drawn reduced stress von Mises on the TOP surface is shown in Figures 13, 14 and 15. The location of plastic hinges is clearly visible (the area where the reduced stress reached the yield stress of material). Evaluation of results follows.

Limit acceleration

$$a_{xL} = LF_L \cdot a_x = 1.83 \cdot 29.43 = 53.85\,ms^{-2} \tag{8}$$

Allowable acceleration

$$a_{xALL} = \frac{a_{xL}}{S_f} = \frac{53.85}{2} = 26.93\,ms^{-2} \tag{9}$$

Strength condition

$$a_x = 29.43\,ms^{-2} > a_{xALL} = 26.93\,ms^{-2} \quad (10)$$

$\Rightarrow$ does not satisfy

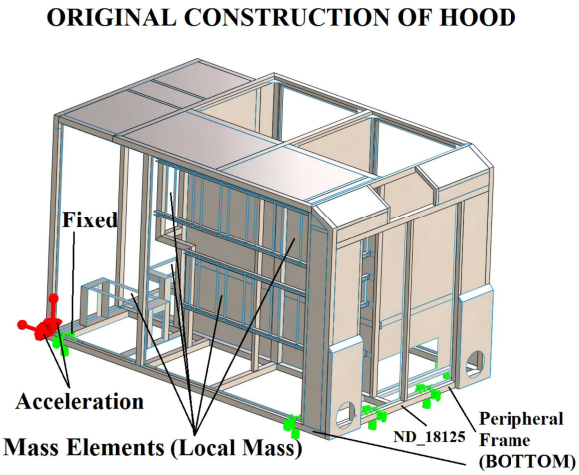

Fig. 10 Numerical model LC2

The calculation result shows that the original hood is not properly designed and the strength condition does not satisfy for the calculation load case $a_z = 1g = 9.81\,\mathrm{ms}^{-2}$ and $a_x = 3g = 29.43\,\mathrm{ms}^{-2}$ (LC2). The original construction of the hood was composed of many types of rectangular tubes. All load were carried only by massive peripheral frame at the bottom of the hood (see Figure 10). Limit state of plasticity occurred after the creation of plastic hinge in a massive peripheral frame. The further parts of the hood are not involved into carrying capacity. Strength conditions were not fulfilled. Limit and allowable loads for all load cases are given in Table 3.

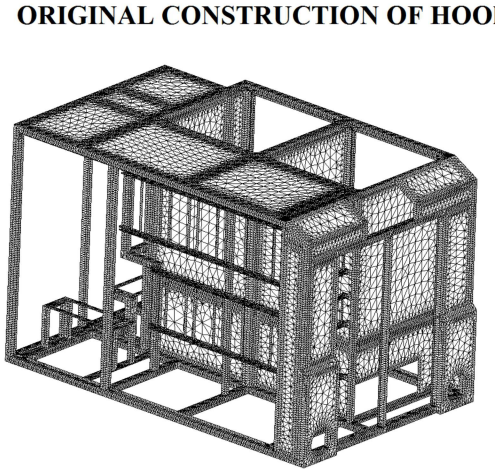

Fig. 11 FEM element mesh LC2

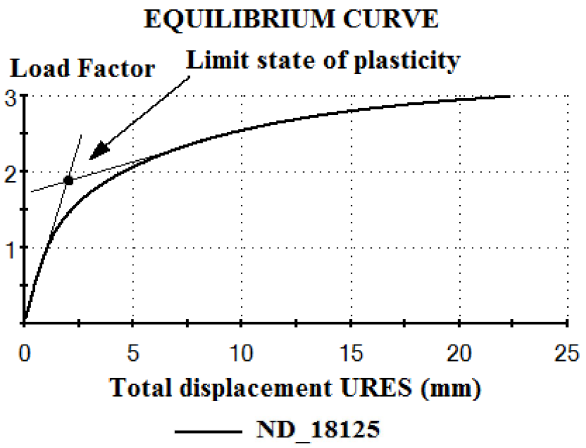

Fig. 12 Equilibrium curve

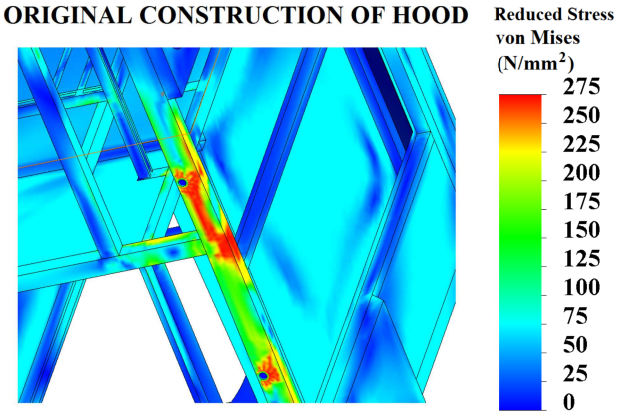

Fig. 13 Limit state of plasticity ($LF = 1.83$) Detail of plastic hinge

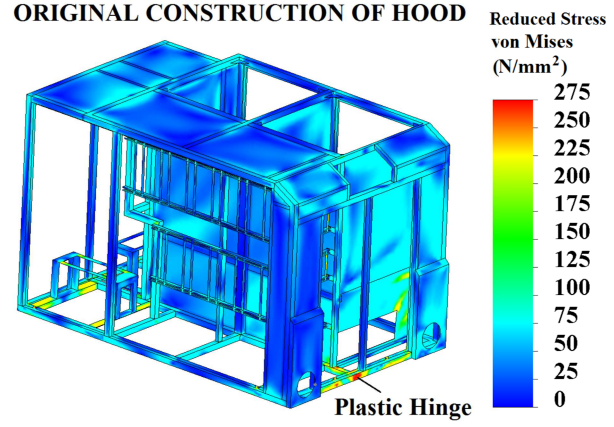

Fig. 14 Limit state of plasticity ($LF = 1.83$) LC2

Table 3 Limit and allowable acceleration for all load cases original construction of hood

load case (LC)	limit acceleration a_L $[\mathrm{ms}^{-2}]$	allowable acceleration a_{ALL} $[\mathrm{ms}^{-2}]$	-	computational acceleration a $[\mathrm{ms}^{-2}]$
LC1	$a_{zL} = 51.22$	$a_{zALL} = 25.61$	$<$	$a_z = 29.43$
LC2	$a_{xL} = 53.85$	$a_{xALL} = 26.93$	$<$	$a_x = 29.43$
LC3	$a_{zL} = 25.90$	$a_{yALL} = 12.95$	$\geq$	$a_z = 9.81$

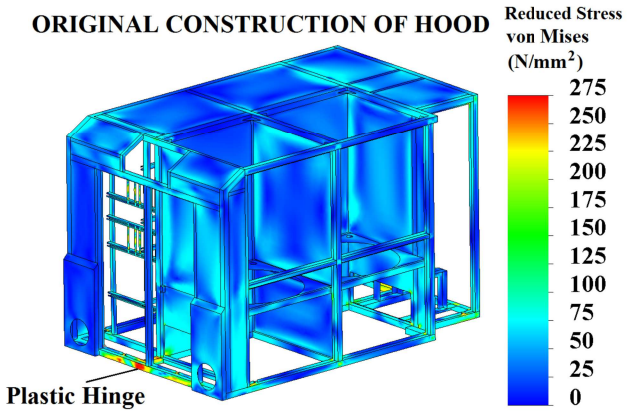

Fig. 15 Limit state of plasticity ($LF = 1.83$) LC2

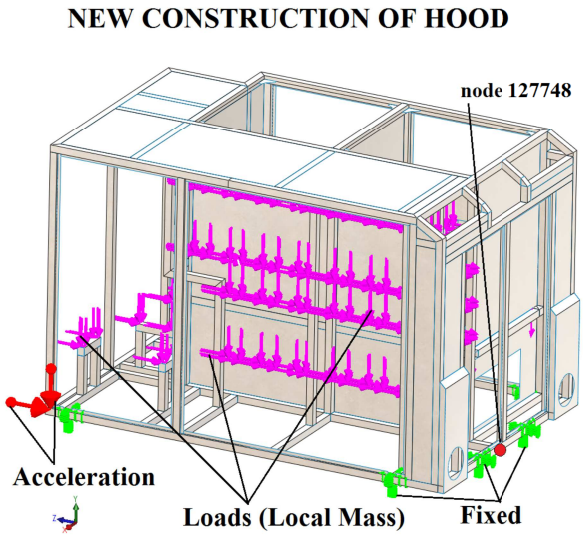

Fig. 16 Numerical model LC2

5 New construction of the hood

The new construction of the hood is composed by single type of square tube of dimensions 60x60x4. The material of the original square tubes S275J2H is changed to S235JRH. The new material has a lower yield strength and ultimate strength, but it is cheaper and more readily available from suppliers of square tubes. Mechanical properties for material S235JRH are given in Table 4. New square tubes have a lower carrying capacity than the peripheral frame (see Figure 10) of the original hood, but it has a higher carrying capacity than other parts of the original hood. Then the whole structure is then involved in the carrying capacity. Limit state of plasticity occurs to the creation of more plastic hinges than the original construction. A brief description of the calculation for selected load case LC2 is shown in this Chapter. Limit and allowable loads for all load cases are given in Table 5.

Table 4 Mechanical properties of material S235JRH

T [°C]	E $[\mathrm{Nmm}^{-2}]$	f_y $[\mathrm{Nmm}^{-2}]$	f_u $[\mathrm{Nmm}^{-2}]$
20	2.01E+5	235	360

5.1 Nonlinear numerical analysis GMNA of new construction

The computational model is shown in Figure16. Local masses (contactors, cooling units) are prescribed by forces. Different methods of prescribed of local masses were used to convergence of the numerical analyzes. FEM mesh is created by shell element SHELL6T. The numerical model is exposed to acceleration $a_z = 1g = 9.81\,\mathrm{ms}^{-2}$ and $a_x = 3g = 29.43\,\mathrm{ms}^{-2}$. Limit state of plasticity is reached in the 16^{th} step. The value of limit load factor is $LF_L = 3.2$ (see equilibrium curve in Figure 17). Deformed models with drawn reduced stress von Mises on the TOP surface are shown in Figures 18, 19, 20 and 21. The location of plastic hinges is clearly visible (the area where reduced stress reached the yield stress of material). Evaluation of the results follows.

The hood of diesel electric locomotive is thin walled construction. Therefore, it is also important to explore area of the equilibrium curve after reaching the first limit state. Then the whole process of the deformation of structure is described and the eventual loss of stability of the thin wall construction can be detected. The equilibrium curve (see Figure 17) indicates that the both types of limit states occurs during deforming of

Table 5 Limit and allowable acceleration for all load cases original construction of hood

load case (LC)	limit acceleration a_L $[\mathrm{ms}^{-2}]$	allowable acceleration a_{ALL} $[\mathrm{ms}^{-2}]$	-	computational acceleration a $[\mathrm{ms}^{-2}]$
LC1	$a_{zL} = 98.30$	$a_{zALL} = 49.15$	$\geq$	$a_z = 29.43$
LC2	$a_{xL} = 94.18$	$a_{xALL} = 47.09$	$\geq$	$a_x = 29.43$
LC3	$a_{zL} = 52.39$	$a_{yALL} = 26.20$	$\geq$	$a_z = 9.81$

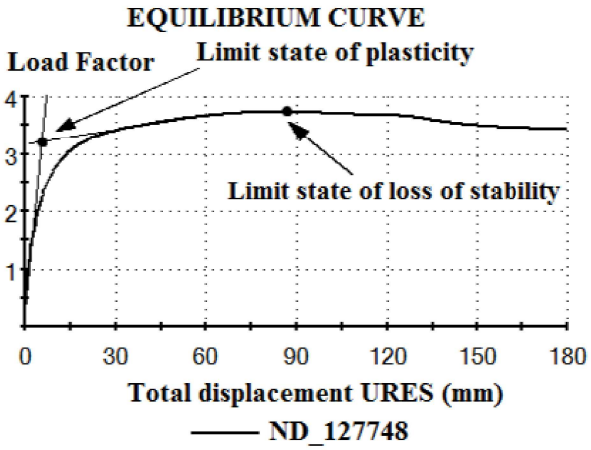

Fig. 17 Equilibrium curve

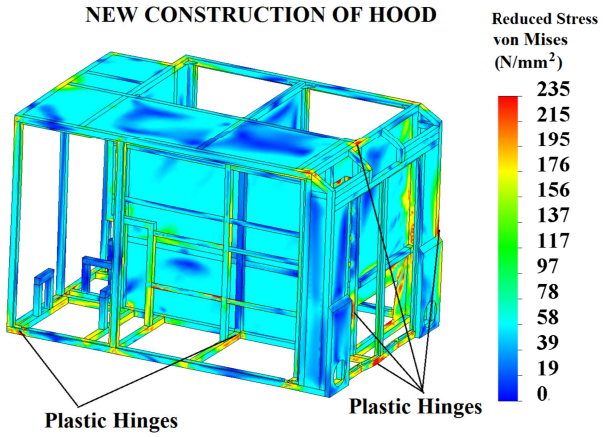

Fig. 18 Limit state of plasticity ($LF = 3.2$) LC2

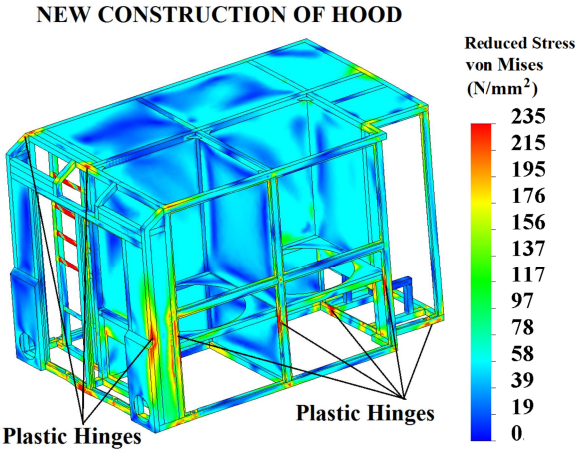

Fig. 19 Limit state of plasticity ($LF = 3.2$) LC2

the numerical model. The first limit state of plasticity is reached when limit load factor $LF_L = 3.2$. The second limit state (loss of stability) is achieved when the limit load factor is $LF_L = 3.74$. The European standard EN 12663-1 [1] recommends using of safety factor $S_3 = 1.5$ for evaluating the limit state loss of stability. The limit state loss of stability occurs up to large deformation of the structure in this numerical model. A small decrease of the carrying capacity of the structure follows after loss of stability (see Figure 17). Using the safety factor S_3 anchored in European standard EN 12663-1 [1] for evaluating loss of stability is sufficient in this case. Limit acceleration for limit state loss of stability

$$a_{xL} = LF_L \cdot a_x = 3.74 \cdot 29.43 = 110.07\,\mathrm{ms}^{-2} \qquad (11)$$

Allowable acceleration for limit state loss of stability

$$a_{xALL} = \frac{a_{xL}}{S_3} = \frac{110.07}{1.5} = 73.37\,\mathrm{ms}^{-2} \qquad (12)$$

Here it is seen that the allowable acceleration for limit state of loss of stability $a_{xALL} = 73.37\,\mathrm{ms}^{-2}$ is higher than allowable acceleration for limit state plasticity $a_{xALL} = 49.15\,\mathrm{ms}^{-2}$ (from Table 5). Therefore, the allowable acceleration of construction is determined from the limit state of plasticity. Another case occurs when the first limit state is the loss of stability. Alternatively, if decrease of carrying capacity after the loss of stability is significant. Then it is better to use the methods anchored in [5–8] for evaluation the loss of stability.

Whole process of deformation of the structure is shown in Figures 18,19,20,21,22 and 23.

6 Conclusion

The strength of the hood was evaluated by two methods. The first methodology is anchored in EN 12663-1 [1]. Evaluation of strength of hood was performed on the basis of pseudo elastic reduced stress on the TOP

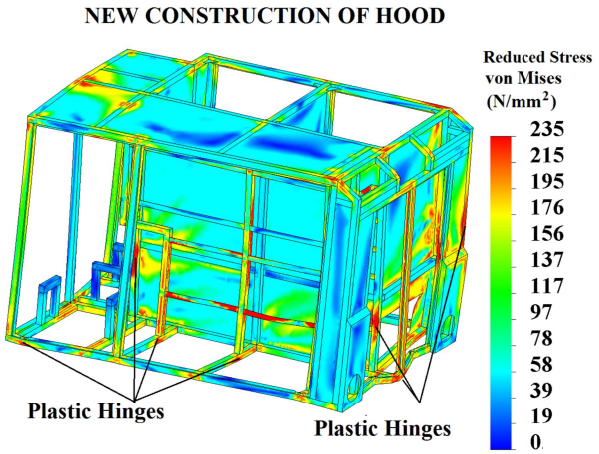

Fig. 20 Limit state of loss of stability ($LF = 3.74$) LC 2

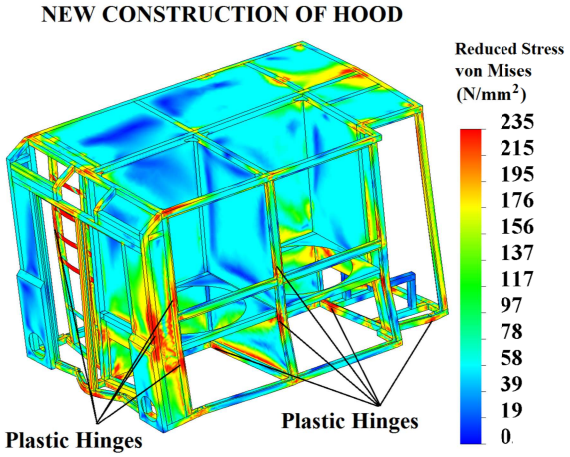

Fig. 21 Limit state of loss of stability ($LF = 3.74$) LC 2

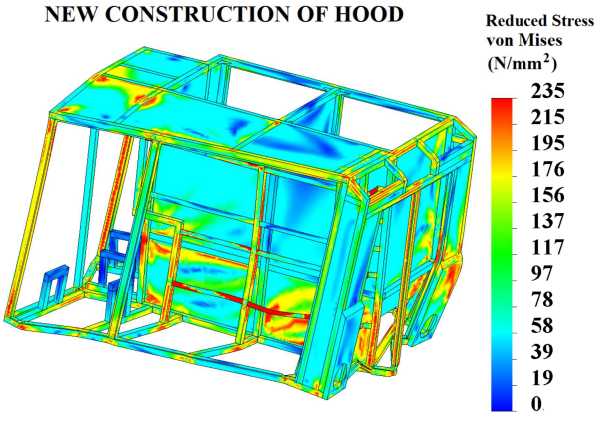

Fig. 22 Reduced stress - end of solution (step 500) LC2

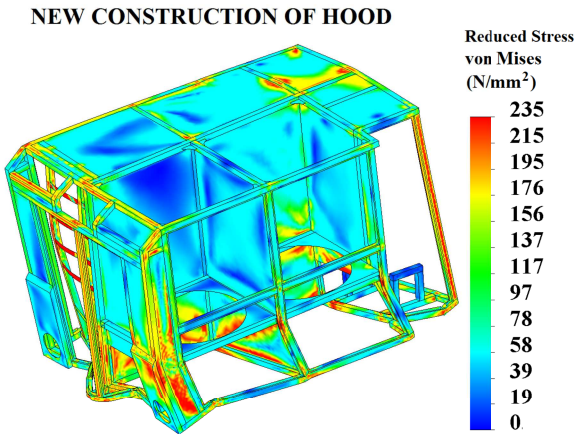

Fig. 23 Reduced stress - end of solution (step 500) LC2

area or BOTTOM area. This method does not properly evaluate the influence of loss of stability and plasticity of carrying capacity structure.

The second methodology is based on the result of geometrically and materially nonlinear numerical analysis. The strength of construction is evaluated from the limit load, when it occurs the real limit state. The real limit states (plasticity and loss of stability) were investigated using nonlinear numerical analyses GMNA. Evaluation of strength of hood was performed on the basis of real limit state of construction.

The results are shown in chapter 4.1 and chapter 5.1. The calculation result shows that the original construction of hood were not properly designed. These results were used to perform the modification of the hood. Strength of new construction was checked by nonlinear numerical analysis GMNA. Fictitious safety factor $S_f = 2$ and nonlinear numerical analysis GMNA were used to evaluate the strength of the hood. The original construction of the hood was composed of many types of rectangular tubes. The new construction of the hood is composed by single type of square tubes 60x60x4. Then the whole structure is involved in the carrying capacity. Limit state of plasticity occurs to the creation of more plastic hinges than the original construction. Carrying capacity of the new construction of hood was verified by a numerical analysis. The carrying capacity of the new construction is higher than the original construction of hood (see limit and allowable loads in Tables 3 and 5).

Fictitious safety factor $S_f = 2$ and nonlinear numerical analysis GMNA are not anchored in EN 12663-1 [1]. Application of nonlinear analysis together with fictitious safety factor for the evaluation of the hood is based on current knowledge of science and technology[8].

Weights of the original and the new construction of the hood are approximately equal. The material of new square tubes is S235JRH. This material is cheaper than original material. Production of the new construction the hood is much more simpler than original construction and economically advantageous.

References

1. EN 12663-1, Railway applications Structural requirements of railway vehicle bodies Part 1: Locomotives and passenger rolling stock. Czech Standards Institute, 2010. (in Czech)
2. FEM Computer program SolidWorks/Simulation (COSMOSWorks) 2014 - Advanced Professional. SolidWorks Corporation
3. EN 1993-1, Design of steel structures. European Standards, (2006)
4. Paščenko P., Stability of thin-walled shell structures in transport technology, Habilitation thesis, University of Pardubice Pardubice, (2009)
5. Esslinger, M.,Geier, B., Postbuckling Behavior of Structures, Springer-Verlag, Wien-New York. ISBN 3-211-81369-1, Udine, (1975)
6. Bushnell D., Computerized buckling analysis of shells, Martinus Nijhoff Publishers, ISBN 90-247-3099-6, Dordrecht (1985)
7. Křupka, V., Paščenko, P., Influence of imperfection on the Snap-Through of Flat Conical Roof Stiffened by Meridional Stringers, Thin-Walled Structures 23, Elsevier Science Limites, ISSN 0263-8231, pp 123-130, (1995)
8. ECCS Buckling of Steel Shells, European Design Recommendations, Fifth edition, Published by ECCS, ISBN 92-9147-000-92, (2008)
9. Volmir, A. C., Flexible Plates and Shells, (in Russian), State Publishing House of Technical/Theoretical Literature, Moscow, (1956)